Twin-emitter design strategy for use in solution-processable thermally activated delayed fluorescence organic light-emitting diodes

Ettore Crovini,[‡a] Zhen Zhang,[‡b] Yu Kusakabe,[c] Yongxia Ren,[c] Yoshimasa Wada,[c] Bilal A. Naqvi,[d] Prakhar Sahay,[d] Wolfgang Brütting,[d] Katsuaki Suzuki,[c] Hironori Kaji,*[c] Stefan Bräse*[b,e] and Eli Zysman-Colman*[a]

[a] Organic Semiconductor Centre, EaStCHEM School of Chemistry, University of St Andrews, St Andrews, Fife, KY16 9ST, UK. E-mail: eli.zysman-colman@st-andrews.ac.uk; Web: http://www.zysman-colman.com; Tel: +44 (0)1334 463826

[b] Institute of Organic Chemistry, Karlsruhe Institute of Technology (KIT), Fritz-Haber-Weg 6, 76131 Karlsruhe, Germany. E-mail: braese@kit.edu; Fax: (+49)-721-6084-8581; Tel: (+49)-721-6084-2903

[c] Institute for Chemical Research, Kyoto University, Uji, Kyoto 611-0011, Japan. E-mail: kaji@scl.kyoto-u.ac.jp

[d] Experimental Physics IV, Institute of Physics, University of Augsburg, Universitätstrasse. 1, 86159 Augsburg, Germany.

[e] Institute of Biological and Chemical Systems – Functional Molecular Systems (IBCS-FMS), Karlsruhe Institute of Technology (KIT), Hermann-von-Helmholtz-Platz 1, D-76344 Eggenstein-Leopoldshafen, Germany

‡ Ettore Crovini and Zhen Zhang contributed equally to this work.

Abstract

In this work we showcase the emitter **DICzTRZ** in which we employed a twin-emitter design of our previously reported material, **ICzTRZ**. This new system presented a red-shifted emission at 488 nm compared to that of **ICzTRZ** at 475 nm and showed a comparable photoluminescence quantum yield of 57.1% in a 20 wt% CzSi film versus 63.3% for **ICzTRZ**. The emitter was then incorporated within a solution-processed organic light-emitting diode that showed a maximum external quantum efficiency of 8%, with Commision Internationale de l'Éclairage coordinate of (0.21, 0.47), at 10 cd m^{-2}.

Keywords: TADF emitters, indolocarbazole, triazine, dimer, blue emitters, orientation, outcoupling effect, solution-processed OLEDs.

Introduction

Organic thermally activated delayed fluorescence (TADF) materials have elicited tremendous excitement as an alternative to phosphorescent complexes as organic light-emitting diodes (OLEDs) because these organic compounds can also achieve a theoretical 100% internal quantum efficiency (IQE) but do not require the use of scarce, noble metals.[1] Since the luminescence in an OLED is achieved through the radiative decay of electrically generated excitons, high-efficiency devices must be able to harvest both the 25% singlet and 75% triplet excitons to produce light.[2] Distinct from phosphorescent compounds, TADF molecules harvest triplet excitons by converting them into emissive singlets via a reverse intersystem crossing (RISC) mechanism. This mechanism is operational when the energy gap (ΔE_{ST}) between the lowest-lying singlet and triplet excited states (S_1 and T_1) is sufficiently small and spin-orbit coupling (SOC) is non-negligible.[3–6] This small ΔE_{ST} can be achieved by spatially separating the highest occupied molecular orbital (HOMO) and the lowest unoccupied molecular orbital (LUMO), thereby reducing the exchange integral of these two orbitals determining the energies of the S_1 and T_1 states relative to the ground state. Also note that due to their spatial separation, these states and their transitions to the ground state have predominantly charge transfer (CT) character. Highly twisted donor-acceptor architectures are typically employed to realize small ΔE_{ST}.[3,7] SOC can be enhanced by ensuring that the nature of the S_1 and T_1 states is different, for example by additionally involving a third (local) triplet state with different symmetry, because otherwise SOC vanishes when the orbital types for these two states are the same, according to El-Sayed's rule.[8]

Indolocarbazole (**ICz**) based emitters have been recently employed in several high-performance and highly horizontally oriented materials. ICz acts as a weak, planar, and rigid donor.[9,10] Examples of compounds incorporating an ICz unit include reports from Xiang *et al.* with the emitters **IndCzpTr1** and **IndCzpTr2**,[11] and Maeng *et al.* with the emitter **TRZ-TPDICz** (Figure **1**).[12] In the doped film, **IndCzpTr1** and **IndCzpTr2** present high photoluminescence quantum yields, Φ_{PL}, of 75.2% and 71.9%, respectively, and delayed fluorescence lifetimes, τ_d, of 25.48 μs and 34.31 μs, respectively. The devices produced with these materials reached maximum external quantum efficiencies (EQE_{max}) values of 14.5% and 30% at low brightness, but efficiency roll-off was significant, with

EQE at 100 cd m^{-2}, EQE_{100}, of 11.0% and 15.3% for the OLEDs with **IndCzpTr1** and **IndCzpTr2,** respectively. The addition of two phenyl units on the ICz in **TRZ-TPDICz** increased the donor strength and led to Φ_{PL} of near unity (96%) and a much shorter τ_d of 8.57 μs in 20 wt% DBFPO film (DBFPO = 2,8-bis(diphenylphosphine oxide) dibenzofuran). The device made from this material has a very high EQE_{max} of 30.3%, which decreases to 18.4% at 1000 cd m^{-2}; the use of a stronger donor in **TRZ-TPDICz** results in a red-shift of the electroluminescence, compared to **IndCzpTr1** and **IndCzpTr2** (the electroluminescence maximum wavelength, λ_{EL} of 472 nm and 496 nm for **IndCzpTr1** and **IndCzpTr2**, respectively, against λ_{EL} of 509 nm for **TRZ-TPDICz**). In our previous work, we presented the first example of a di-functionalized ICz-based emitter **ICzTRZ**,[13,14] that presented nearly complete horizontal orientation in a wide number of host matrices. The best combination of properties was obtained in mCBP as a host, with the photoluminescence maximum wavelength, λ_{PL} of 479 nm, Φ_{PL} of 70%, and a τ_d of 121.1 μs. The anisotropy factor (a) in 5 wt% mCBP film is 0.09, indicating a very high degree of horizontal orientation (91%), which together with the high quantum yield led to a high-performing device with EQE_{max} of 22.1%.

It has been documented in the literature that some multichromophore emitters show enhanced molar extinction coefficients of absorption and high Φ_{PL} .[15–20] This led to OLEDs employing dual or multi emitter-designed compounds to show much improved EQE_{max} compared to devices with their single-emitter counterparts (Figure **1**), albeit with a red-shifted emission.[18–21] The advantages of the dual-emitter design are best illustrated by the cross-comparison of **CzTRZ**,[22,23] a molecule that did not present any TADF and thus the OLED showed a low EQE_{max} of 5.8%, while the emitter, **33TCzTTrz**,[24] is TADF and the OLED showed a much superior EQE_{max} of 25.0%. There is a significant red-shift of the electroluminescence, with λ_{EL} going from 449 nm for **CzTRZ** to 490 nm for **33TCzTTrz**.

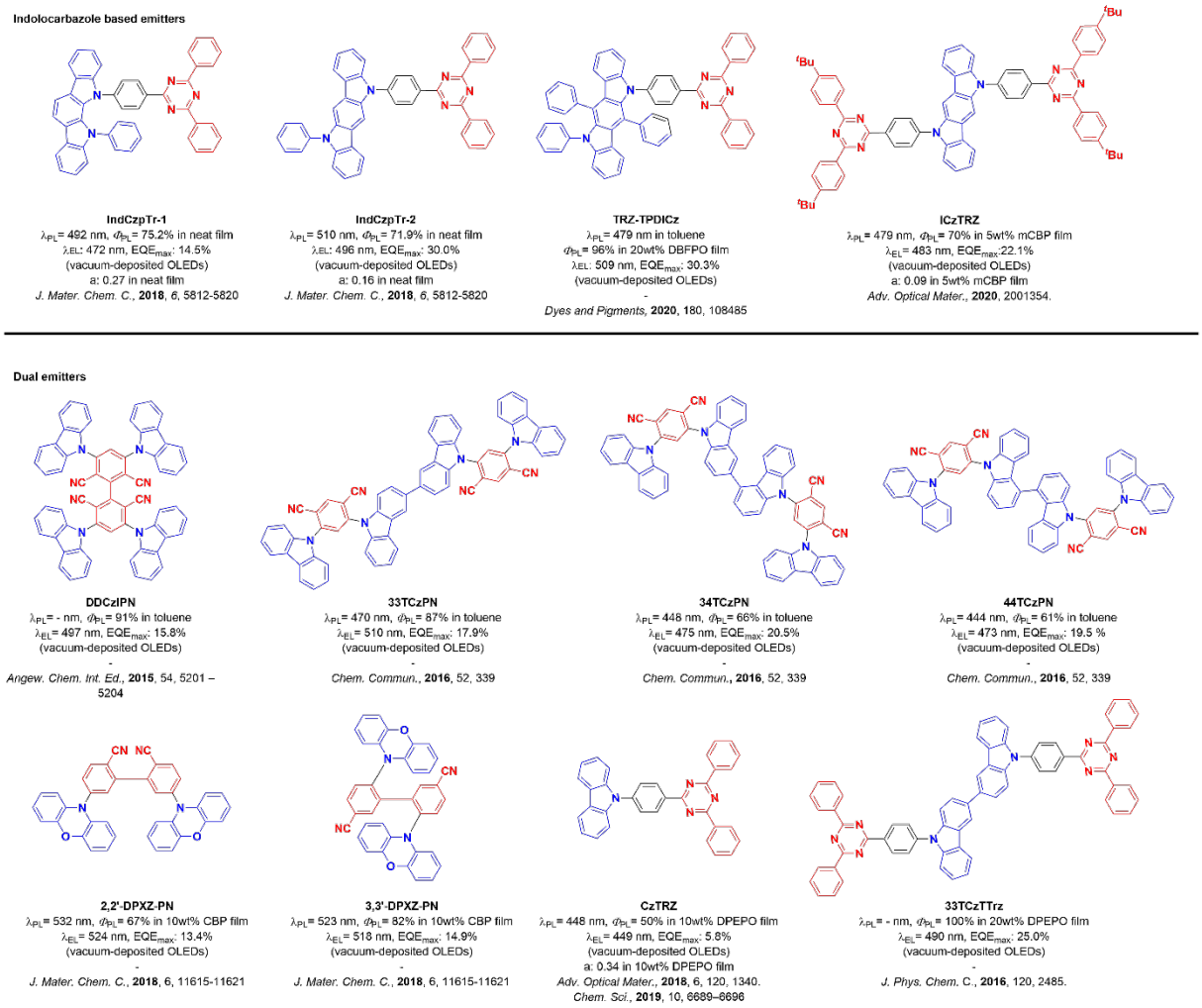

Figure **1**. Molecular structures of emitters.

In this work, we utilized a similar strategy to assess the change in optoelectronic properties and device performance of the compound **DICzTRZ** compared to our recently reported **ICzTRZ** study.[14] We note that the effective doubling of the molecular weight necessitates that we fabricate solution-processed devices. Importantly, solution-processed films tend to present isotropic orientation[25] due to the slower deposition times coupled with higher degree of freedom of movement in the solution, unlike the orientation of the emitter in vacuum-deposited films, which occurs only at the surface of the film where the emitter orientation is then "frozen" into place once additional layers of material have covered it. While this loss of controlled orientation in the solution-processed film is true for small molecules, polymers and other high molecular weight emitters can show at least some degree of orientation in solution-processed films. For instance, Senes *et al.*[26,27] showed that the **OPVn** series of polymers exhibited higher horizontal orientation by

increasing the length of the polymer chain, and by extension the molecule. Considering the high degree of horizontal orientation that **ICzTRZ** already showed in vacuum-deposited films (anisotropy factor of 0.09 in 10 wt% film of mCBP) and the high molecular weight of **DICzTRZ**, we hypothesized that **DICzTRZ** may also present horizontal orientation in the film and subsequently improve light outcoupling in the device.

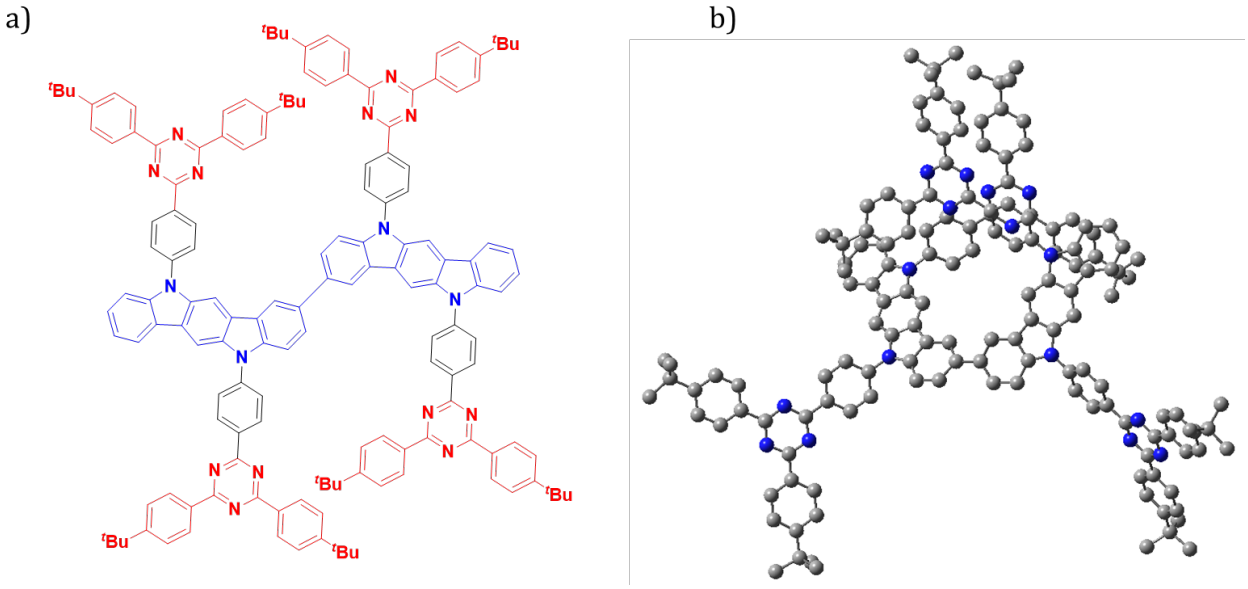

Figure **2**. a) Molecular structure and b) optimized DFT-calculated geometry of **DICzTRZ**.

Synthesis

The oxidative coupling conditions for the synthesis of carbazole dimers were initially applied to access the dimer of **ICzTRZ**.[28,29] Treating **ICzTRZ** with $FeCl_3$ in DCM at room temperature for 12 hours did not lead to any product formation. However, when the temperature was increased to 40 °C, **DICzTRZ** was formed and was isolated in a yield of 20%, while increasing the temperature to 60 °C resulted in complete consumption of the starting material and **DICzTRZ** was isolated in 66% yield. The identity and purity of **DICzTRZ** were determined by a combination of NMR spectroscopy, mass spectrometry, and IR spectroscopy.

Theoretical calculations

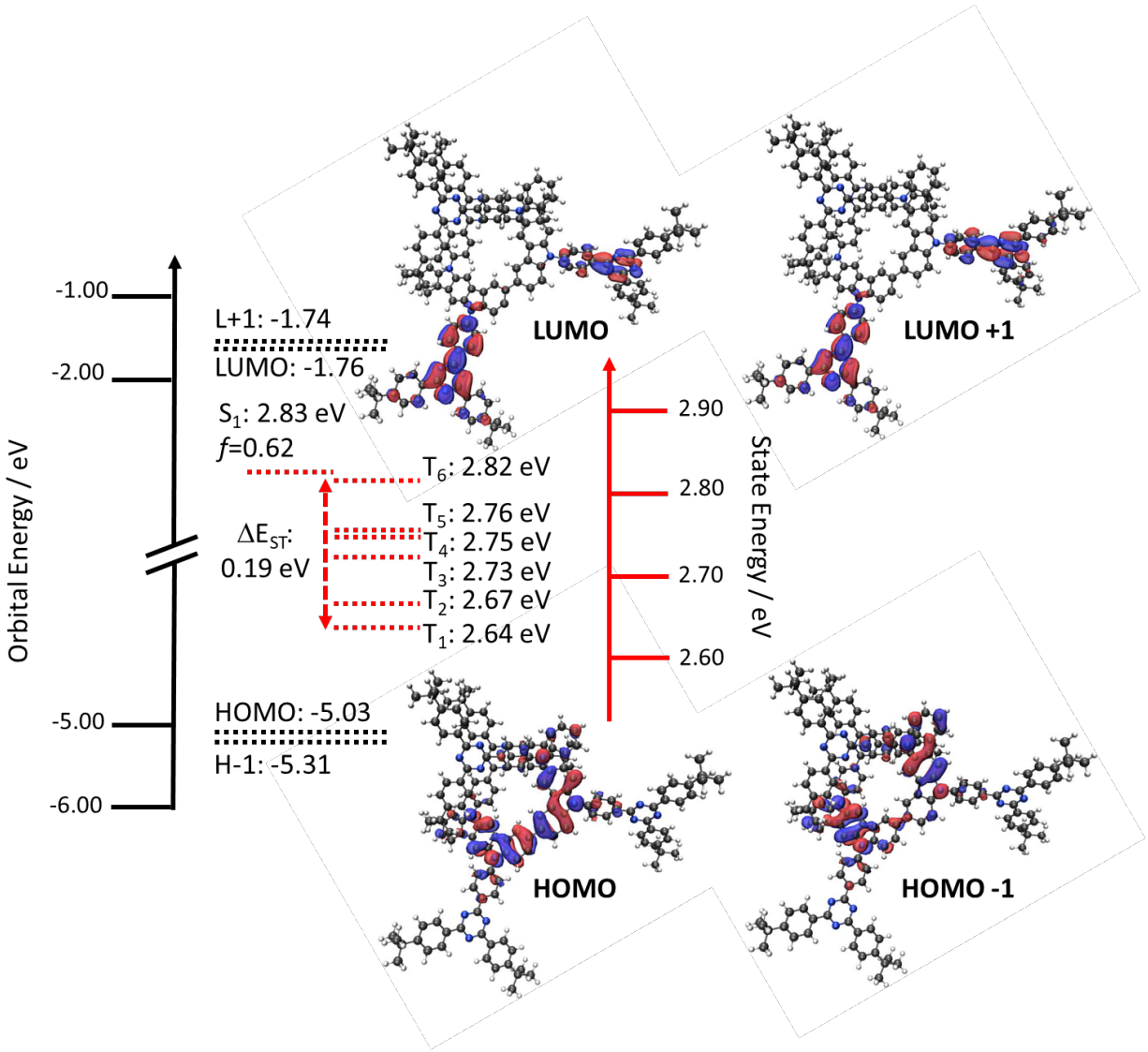

Figure **3**. HOMO, HOMO−1 (H−1), LUMO, and LUMO+1 (L+1) electron density distributions (isovalue: 0.02) and energy levels, excited state energy levels.

Density functional theory (DFT) and time-dependent DFT (TD-DFT) calculations in the gas phase at the PBE0/6-31G(d,p) level reveal the potential of **DICzTRZ** as a TADF material (Figure **3**). The nature of the S_1 and T_1 states and their corresponding energies were then obtained using the Tamm-Dancoff approximation[30] to TD-DFT (TDA-DFT). **DICzTRZ** possesses a ΔE_{ST} of 0.19 eV, comparable to 0.22 eV obtained for **ICzTRZ** at the same level of theory. We can observe a slightly stabilized S_1 energy of 2.83 eV (2.92 eV for **ICzTRZ**) and T_1 energy of 2.64 eV (2.70 eV for **ICzTRZ**)[14] compared to those of **ICzTRZ**. Compared to **ICzTRZ,** there is a much higher density of intermediate triplet states between S_1 and T_1, which is expected to enhance the efficiency of the RISC process due to

the presence of increased spin-vibronic coupling.[31–36] The permanent dipole moment (PDM) of **DICzTRZ** is substantial increased to 2.1 Debye compared to that in **ICzTRZ** (0.3 Debye); however, both the transition dipole moment (TDM) and oscillator strength (*f*) are slightly smaller (TDM = 7.6 Debye and *f* = 0.62) than the values calculated for **ICzTRZ** (TDM = 7.9 Debye and *f* = 0.72). **DICzTRZ** shows a shallower HOMO at −5.03 eV, reflective of a certain degree of conjugation between the two indolocarbazole moieties, compared to the HOMO of **ICzTRZ** (−5.19 eV). The LUMO level remains essentially unchanged (−1.76 eV for **DICzTRZ** vs −1.75 for **ICzTRZ**) since the electronic environment surrounding the ^{t}Bu-triazine remains essentially unperturbed.

Optoelectronic properties

The electrochemical properties of the two materials were studied in degassed DCM with tetra-*n*-butylammonium hexafluorophosphate as the electrolyte and Fc/Fc^{+} as the internal reference (Figure **4a**), data are reported versus a Saturated Calomel Electrode (SCE). In both **DICzTRZ** and **ICzTRZ**[14] we observed a reversible oxidation wave with respective oxidation potential (E_{ox}) at 0.87 V and 0.96 V *vs* SCE. Both compounds also present a second oxidation wave that is more prominent and cathodically shifted for **DICzTRZ** at 1.05 V, compared to 1.14 V for **ICzTRZ**. No reduction wave is observed for **DICzTRZ**. The HOMO value calculated from the oxidation potential obtained from differential pulse voltammetry (DPV), is −5.21 eV, which is stabilized compared to that predicted from DFT (E_{HOMO}: −5.03 eV); however, the less positive oxidation potentials in **DICzTRZ** versus **ICzTRZ** does align with the predictions obtained by DFT.

The UV-vis absorption spectrum of **DICzTRZ**, while slightly red-shifted and with higher molar absorptivity (as was the case for previously published multichromophore materials), [15–20] coincides closely with the one from **ICzTRZ**[14] (Figure **4b**) and also with other indolocarbazole-based compounds.[11] The nearly identical profile leads us to conclude that the character of the transitions are likely to be very similar to those associated with **ICzTRZ**, showing CT character for the two absorption bands between 330 and 350 nm, between the diindolocarbazole donor and the two triazine acceptors, while the second lower energy band one presents LE (on the indolocarbazole) character. The two lower energy and lower absorptivity bands at 390 nm and 410 nm are both assigned to CT-type transitions.

Solvatochromic studies (Figure **4c**) for **DICzTRZ** show that the PDM of the ground state structure is small and so the absorption spectrum is essentially not affected by changes in polarity, while the excited state shows the characteristic positive solvatochromism associated with an emission from a CT state (λ_{PL} going from 462 nm in the least polar methyl-cyclohexane to 548 nm in the most polar dichloromethane). From the previously calculated HOMO level determined from DPV and the optical gap obtained from the intersection of the normalized absorption and emission spectra in DCM (E_{gap} = 2.71 eV), we were able to obtain a LUMO value of −2.50 eV.

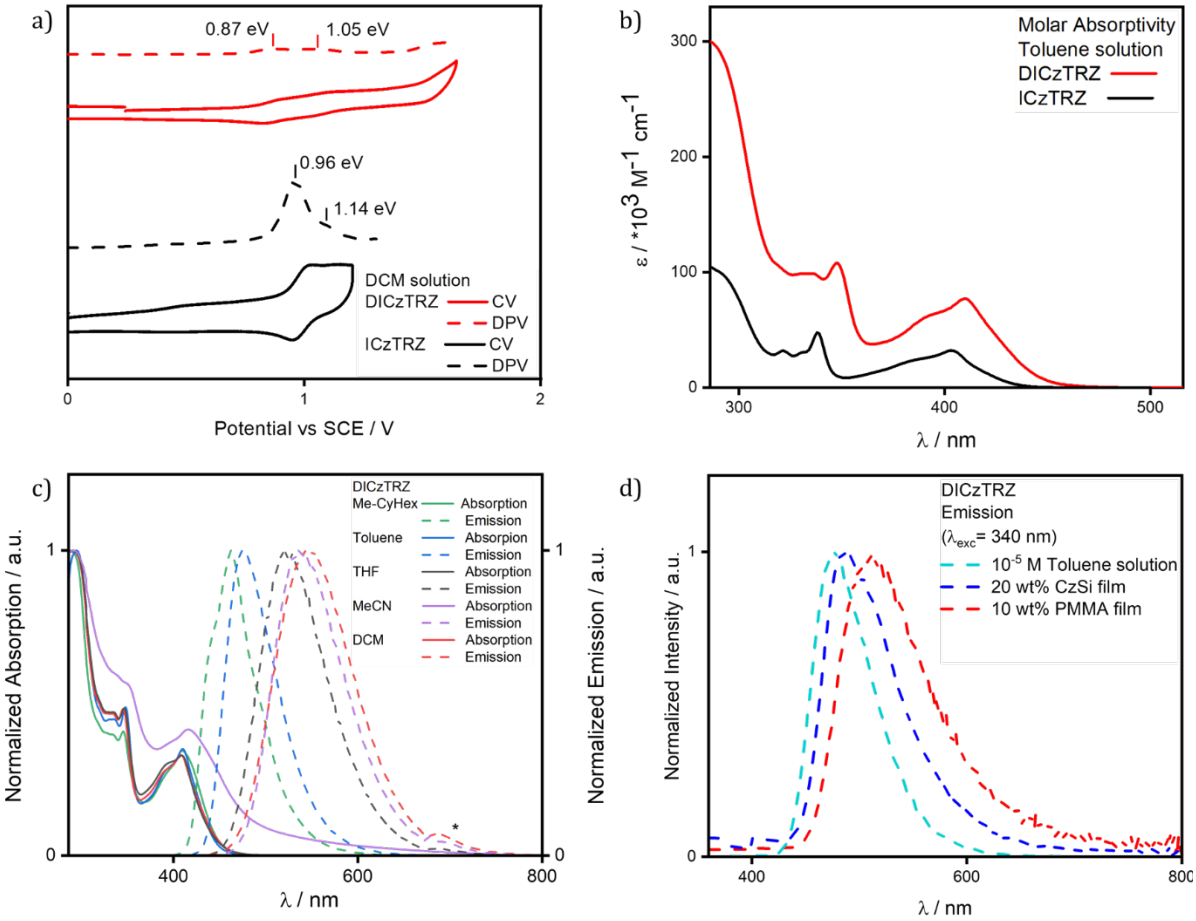

Figure **4**. a) Cyclic voltammetry (CV) and differential pulse voltammetry (DPV) of **DICzTRZ** in DCM (scan rate = 100 mV/s). b) UV-vis absorption spectrum of **DICzTRZ** in 10^{-5} M toluene solution. c) Ground and excited state solvatochromism study of **DICzTRZ** (excitation wavelength, λ_{exc}, = 340 nm, * = second harmonic of the excitation source); d) emission spectra of **DICzTRZ** in 10^{-5} M toluene solution (cyan), 20 wt% CzSi film (blue), and 10 wt% PMMA film (red), (λ_{exc} = 340 nm).

The emission of **DICzTRZ** in degassed toluene is red-shifted at 477 nm compared to **ICzTRZ**,[14] at 462 nm (Figure **4d**). The excitation spectrum mirrors the profile of the UV-vis absorption (Figure **S4a**). Transient PL measurements in degassed toluene show mono-exponential prompt and delayed fluorescence decays at 8.94 ns and 28.83 μs, respectively (Figure **S4c-d**). After exposure to oxygen, the delayed fluorescence disappears while the prompt decay lifetime, τ_p, is slightly reduced to 6.80 ns, implying the involvement of triplet states in the emission. When compared to **ICzTRZ** in degassed toluene, **DICzTRZ** presents comparable τ_p (9.0 ns for **ICzTRZ**), while we observe a substantial one order of magnitude decrease in the delayed lifetime, τ_d, (229.2 μs for **ICzTRZ**[14]), reflective of a more efficient RISC process. **DICzTRZ** is less emissive than **ICzTRZ** (Φ_{PL} of 72%[14]), with Φ_{PL} in degassed toluene of 60% that decreases to 44% once exposed to oxygen. This reduction in Φ_{PL} is in part due to the decrease in the radiative decay rate given the smaller calculated oscillator strength for the emissive S_1 state for this compound compared to **ICzTRZ**. The ΔE_{ST} of **DICzTRZ** in toluene glass at 77 K is 0.21 eV (see Figure **S4**, which is significantly smaller than the 0.32 eV obtained for **ICzTRZ** under the same conditions. The T_1 levels of both **DICzTRZ** and **ICzTRZ** are comparable at 2.59 eV and 2.62 eV, respectively, while the S_1 level for **DICzTRZ** is more stabilized at 2.80 eV vs 2.94 eV for **ICzTRZ**). We can clearly observe that the phosphorescence spectrum presents a well-defined structure, typical for transitions coming from a local excited (LE) type state on the di-indolocarbazole. TDA-DFT calculations in the gas phase predict that the T_1 state is CT in nature while the lowest-lying triplet states with LE character are T_3 and T_4 (T_3 and T_4 are at 2.73 eV and 2.75 eV, respectively, while T_1 is at 2.64 eV, See Table **S1** and Figure **S3**. The character of the different transitions was also evaluated by analysis of the Natural Transition Orbitals (NTOs) (See Table **S2**). The T_1 and T_2 HONTO and LUNTO (Highest Occupied and Lowest Unoccupied Natural Transition Orbitals) are localized on the central di-indolocarbazole and adjacent triazine, respectively, showing a clear CT between donor and acceptor moieties in the molecule. As previously mentioned, T_3 and T_4 present LE character, with the NTOs localized mainly the central di-indolocarbazole. The character of each of T_5 and T_6 is more difficult to assign as the electron density of the transition is localized on one of the indolocarbazole-triazine fragments and showing a high degree of overlap between the HONTO and LUNTO, which indicates a transition with a mixed CT

and LE character. S_1 also presents a clear CT transition from the di-indolocarbazole to the triazine.

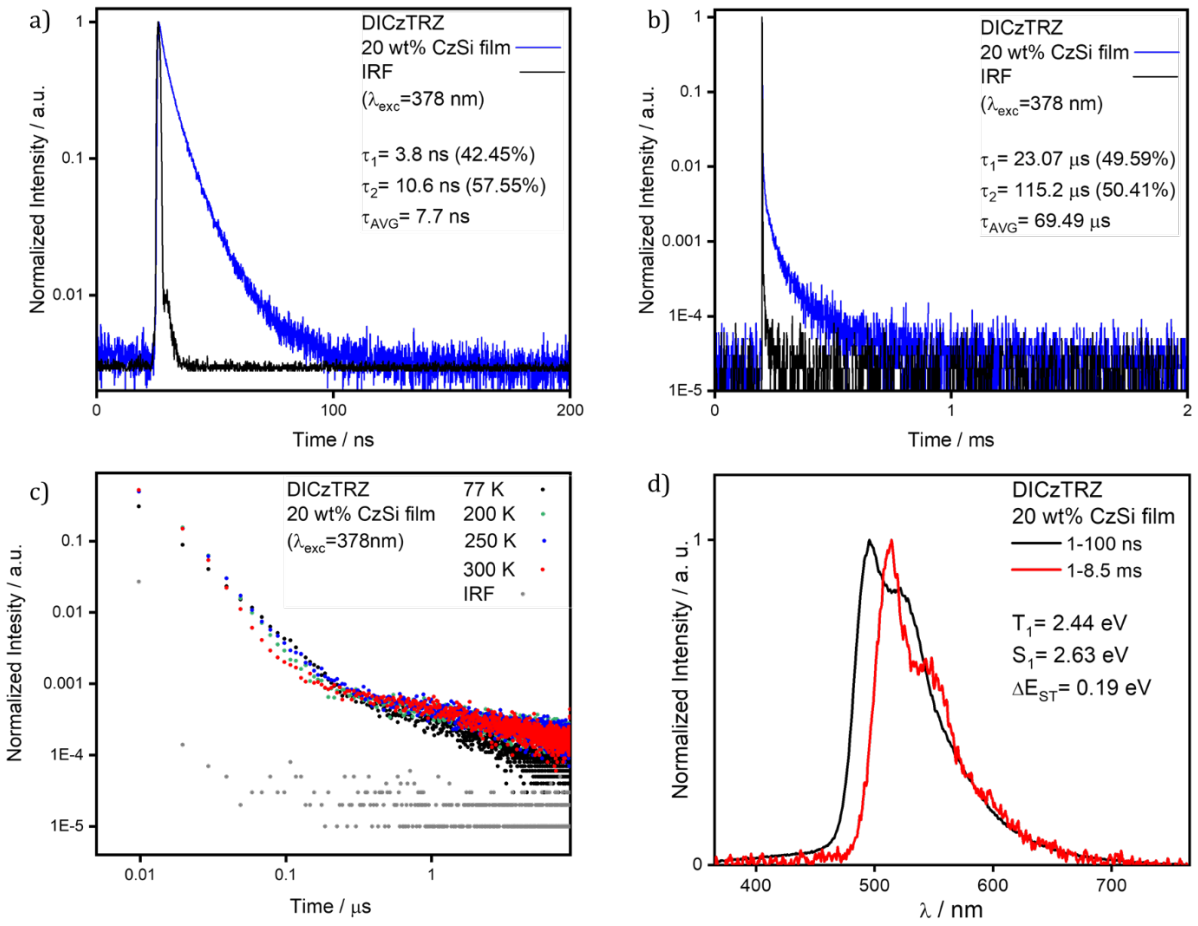

Figure **5.** a) Prompt and b) Delayed time-resolved decay in spin-coated 20 wt% CzSi film of **DICzTRZ** (λ_{exc} = 378 nm); c) Delayed fluorescence decay data measured at different temperatures in spin-coated 20 wt% CzSi film of **DICzTRZ** (λ_{exc} = 378 nm); d) Prompt fluorescence and phosphorescence spectra at 77 K in drop-casted 20 wt% CzSi film (λ_{exc} = 343 nm, prompt and delayed fluorescence spectra were obtained in the 1–100 ns and 1–10 ms time range, respectively).

With a view to incorporating **DICzTRZ** as the emitter in a solution-processed OLED, we next investigated the photophysical behavior of this compound in solid host matrices. We began with 10 wt% doped film of **DICzTRZ** in PMMA as the polarity of PMMA emulates well that of toluene.[37] The emission maximum in PMMA is 514 nm with a corresponding Φ_{PL} of 29% under N_2. The significantly red-shifted emission in the PMMA film compared to that in toluene coupled with a significantly lower Φ_{PL} is suggestive that aggregation-

caused quenching is prevalent in this host matrix. Transient PL measurement (Figure **S5** showed multiexponential decay kinetics and lifetimes with an average τ_p of 8.6 ns [τ_1=3.5 ns (37.5%), τ_2=11.6 ns (62.5%)] and an average τ_d of 156.1 μs [τ_1=27.98 μs (39.5%), τ_2=239.7 μs (60.5%)], respectively. The average prompt fluorescence lifetimes are of a similar magnitude to that of **ICzTRZ** (τ_p = 11.5 ns) while the average delayed fluorescence decays much faster for **DICzTRZ** (τ_d = 252.8 μs for **ICzTRZ**). We next focused on the photophysical study in a suitably high triplet energy small molecule host material, CzSi (9-(4-*tert*-butylphenyl)-3,6-bis(triphenylsilyl)-9*H*-carbazole). The emission in CzSi at 488 nm, is only slightly red-shifted compared to that in toluene. Gratifyingly, the Φ_{PL} is substantially higher at 57% in 20 wt% doped CzSi film, compared to the 10 wt% PMMA films (Table **1**). In this host, transient PL measurements show the presence of both prompt and delayed fluorescence with respective average lifetimes of τ_p 7.7 ns [τ_1=3.8 ns (42.5%), τ_2=10.6 ns (57.6%)] and τ_d of 69.49 μs [τ_1=23.07 μs (49.6%), τ_2=115.2 μs (50.4%)]. While the Φ_{PL} largely benefits from the change in the host, the lifetimes of the prompt fluorescence remain largely unchanged while we observe a much shorter delayed fluorescence. Both prompt and delayed lifetimes of **DICzTRZ** in CzSi are shorter than those of **ICzTRZ** in the same host (τ_p 9.5 ns, τ_d of 147.3 μs). The ΔE_{ST} values in CzSi (Figure **5d**) and PMMA (Figure **S5**), are 0.19 eV and 0.03, respectively. From a cross-comparison of the state energies (Table **1**) we can see that the T_1 state remains essentially the same regardless of the environment, this due to the LE nature of this excited state. The energy of the S_1 state varies with the environments (with energies of 2.94 eV, 2.72 eV, and 2.75 eV for toluene solution, CzSi film and PMMA film, respectively for **ICzTRZ**), characteristic of a CT type state, but the shape of the spectra in all media adopt a structured profile, typical for LE-type states, suggesting a state of mixed CT and LE character (Figure **S4d** and **S5d**). **DICzTRZ** and **ICzTRZ** possess comparable ΔE_{ST} in CzSi, at 0.19 eV and 0.16 eV respectively. Temperature-dependent time-resolved PL decays (Figure **5c**) reveal the clear increase in the intensity of the delayed emission with higher temperature, a hallmark of TADF.

Table **1.** Photophysical properties of **ICzTRZ**[14] and **DICzTRZ**.

Material	**Environment**	λ_{PL} / nm[c]	Φ_{PL} N_2 (air)[d] / %	τ_p, τ_d[g] / ns; µs	S_1[h] / eV	T_1[i] / eV	ΔE_{ST}[i] / eV
ICzTRZ[a]	Toluene (10^{-5} M)	462	72 (56)[e]	9.0; 229.2	2.94	2.62	0.32
	CzSi 20 wt%	475	63 (50)[f]	9.5; 147.3	2.72	2.56	0.16
	PMMA 10 wt%	470	31 (28)[f]	115; 252.8	2.75	2.64	0.11
DICzTRZ[b]	Toluene (10^{-5} M)	477	60 (44)[e]	8.9; 28.83	2.80	2.59	0.21
	CzSi 20 wt%	488	57 (42)[f]	7.7; 69.49	2.63	2.44	0.19
	PMMA 10 wt%	514	29 (22)[f]	8.6; 156.1	2.61	2.58	0.03

[a] previous work [14]; [b] this work; [c] measured at room temperature; [d] λ_{exc} = 340 nm; [e] obtained *via* the optically dilute method[38] (see SI), quinine sulfate (0.5 M) in H_2SO_4 (aq) was used as the reference, Φ_{PL}: 54.6%, λ_{exc} = 360 nm;[39] [f] obtained via integrating sphere; [g] τ_p (prompt lifetime) and τ_d (delayed lifetime) were obtained from the transient PL decay of degassed solution/doped film, λ_{exc} = 378 nm; [h] S_1 was obtained from the onset of the prompt emission measured at 77 K; [i] T_1 was obtained from the onset of the phosphorescence spectrum measured at 77 K; [j] $\Delta E_{ST} = S_1 - T_1$.

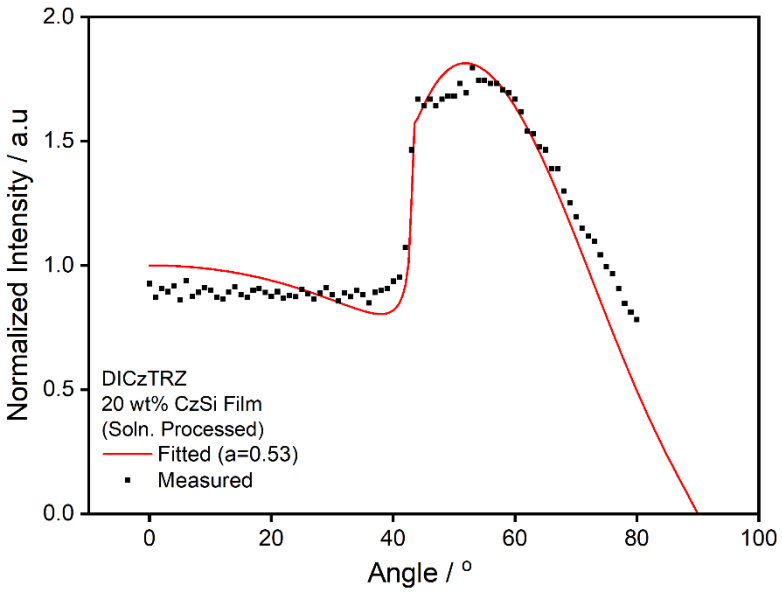

Figure **6**. Angle-resolved photoluminescence measurement of a solution-processed film of 20 wt% **DICzTRZ** in CzSi. The red line shows a fit using the dipole emission model as described in detail in the SI, yielding an anisotropy factor, *a*, of 0.53 (data taken at λ_{em} = 500 nm).

Designing a molecule able to achieve RISC and the desired 100% IQE is just the first step toward an efficient TADF material since the light needs to escape the OLED device. A device is composed of a stack of several layers of different materials (thus with different refractive indexes) between two electrodes that can lead to total internal reflection at the organic-glass as well as the glass-air interfaces and coupling to surface plasmon polaritons (SPP) at the interface with the cathode, lowering the EQE of the device to a

maximum of about 25%. An emitter will emit light perpendicularly to its TDM, which means that creating a structure able to achieve horizontal orientation of the TDMs, quantified by the anisotropy factor, *a*, in the film – where 1- *a* is the fraction of horizontally aligned TDMs, will maximize the amount of light exiting the device.

Polarization and angle dependent luminescence spectroscopy was used to measure *a* for solution processed films of 20 wt% **DICzTRZ** in CzSi (9-(4-*tert*-butylphenyl)-3,6-bis(triphenylsilyl)-9*H*-carbazole). The data were then analysed *via* optical simulation to yield and anisotropy factor of 0.53, which disappointingly implies that the emitter presents a strongly vertical orientation (Figure **6**); the optical simulation of 10 wt% **DICzTRZ** in mCP film is shown in Figure **S6**.

OLED devices

Finally, **DICzTRZ**-based OLEDs were fabricated using the following device structure: ITO (indium tin oxide) (50 nm)/PEDOT:PSS (poly(3,4-ethylenedioxythiophene) polystyrene sulfonate) (35 nm)/PVK (poly(9-vinylcarbazole)) (10 nm)/*X* wt% **DICzTRZ**: CzSi (20 nm)/PPF (2,8-bis(diphenylphosphoryl)dibenzo[b,d]furan) (5 nm)/TPBi (1,3,5-tris(1-phenyl-1*H*-benzo[d]imidazol-2-yl)benzene) (50 nm)/Liq (lithium quinolin-8-olate) (1 nm)/Al (80 nm), where *X* is 20 or 30. The PVK layer is applied to facilitate hole injection from PEDOT:PSS to the emitting layer. Besides, PVK and PPF, possessing high T_1 energies of 3.0 eV[40] and 3.1 eV,[41] respectively, were inserted to confine the excitons in the emitting layer. PEDOT:PSS, PVK and the emitting layer were fabricated by spin-coating, and the other layers were vacuum-deposited. Device characteristics are shown in Figure **7** and the device performance is summarized in Table **2**. As shown in Table **2**, 20 wt% **DICzTRZ**-based OLEDs achieved EQE_{max} of 8.0% and λ_{EL} of 492 nm with CIE coordinates (*x*, *y*) of (0.21, 0.47) at 10 cd m^{-2}.

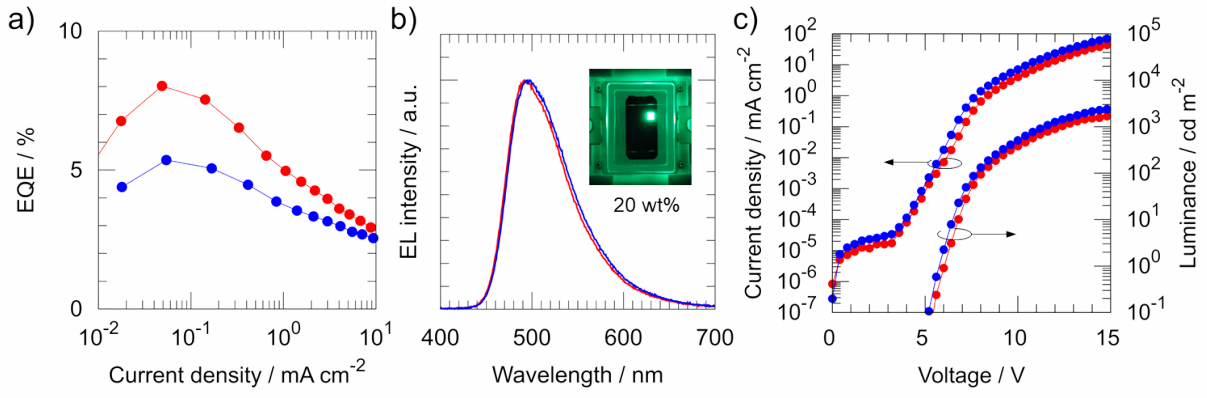

Figure **7**. Device characteristics of 20 and 30 wt% **DICzTRZ**-based OLEDs, which are represented by red and blue, respectively. a) EQE-current density b) EL spectra and c) current density-voltage-luminance properties.

Table 2. Device performances of *X* wt% DICzTRZ-based OLEDs (where *X* = 20, 30).

Concentration / %	EQE_{max} / %	λ_{EL} / nm[a]	CIE (x, y)
20	8.0	492	(0.21, 0.47)
30	5.4	498	(0.22, 0.49)

[a] Determined from EL spectrum at 1 mA cm^{-2}.

We next simulated the device EQE (Figure **S7**). As shown in Figure 8, with the pre-determined parameters (Φ_{PL} and a) along with the optical constants of the different materials in the OLED stack, we predict the device to show an EQE_{max} of 9%, which aligns with the measured EQE_{max}. The simulation also demonstrates that at the given Φ_{PL} of 57.1%, a device EQE in the range of 10% is a result of the vertical orientation of the emitter within the EML.

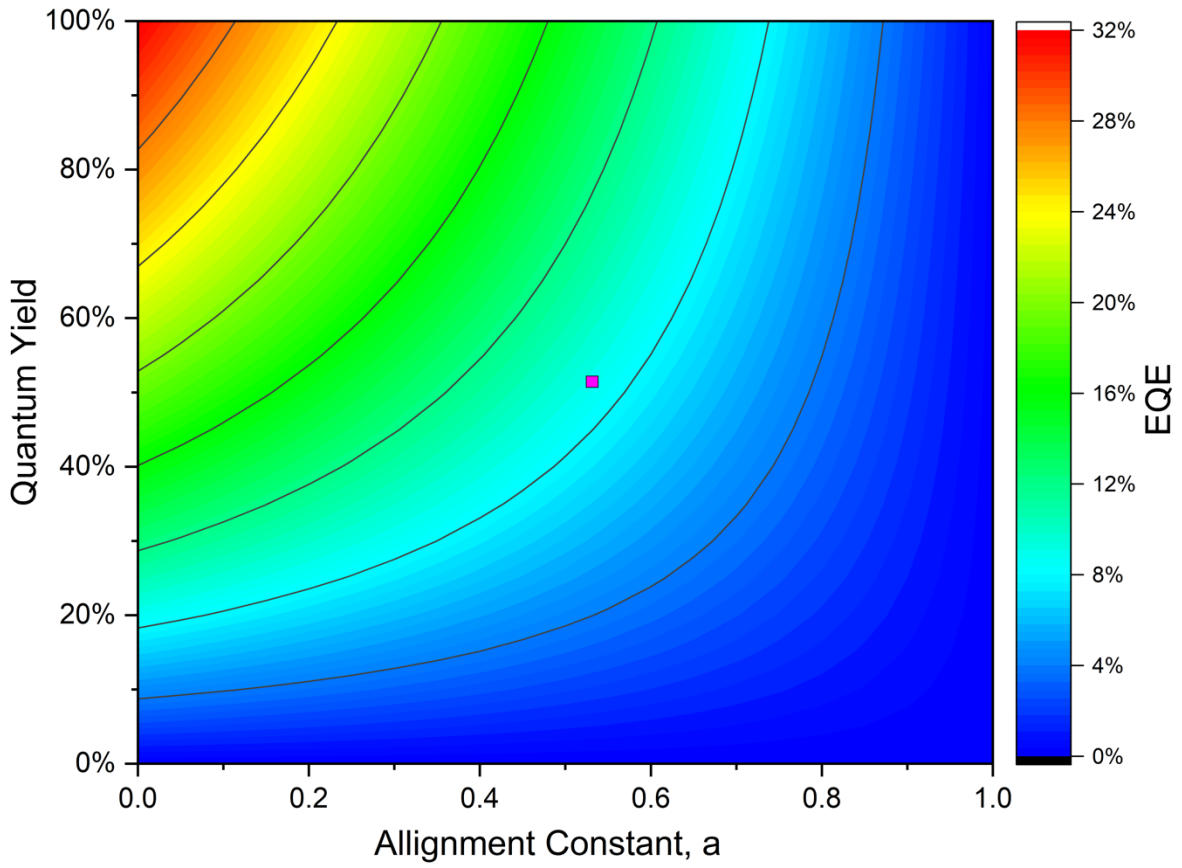

Figure **8**. Device efficiency simulation of fabricated 20wt% **DICzTRZ**-based OLEDs depicting the variation in EQE with varied PL Quantum Yield (vertical axis) and anisotropy factor (horizontal axis). Predicted EQE indicated with a pink rectangular mark which agrees with the experimental results.

Conclusions

Building upon our previously reported emitter, **ICzTRZ**, here we presented a dual emitter strategy consisting of two **ICzTRZ** moieties covalently linked together in the form of **DICzTRZ**. DFT calculations showed a much larger density of triplet states, which suggests that RISC will be faster in this compound compared to its parent. The twin design strategy leads to an enhancement in the molar extinction coefficient of the low-lying CT states, accompanied by a red-shift in the emission. The 20 wt% doped CzSi film of **DICzTRZ** emits in the blue at 488 nm and shows a photoluminescence quantum yield of 57.1%. Unfortunately, the TDM of this material is not preferentially horizontally oriented in the solution-processed film. The OLED shows an EQE_{max} of 8.0% and λ_{EL} of 492 nm.

Supporting information

Synthesis protocols, NMR spectra, supplementary photophysical measurements, computational data obtained from DFT and TD DFT and electroluminescence data.

Acknowledgments

We (EC, BAN, PS, WB & EZ-C) thank EU Horizon 2020 Grant Agreement No. 812872 (TADFlife) for funding. This project is supported by the Helmholtz Association Program at the Karlsruhe Institute of Technology (KIT). The German Research Foundation (formally Deutsche Forschungsgemeinschaft DFG) in the framework of SFB1176 Cooperative Research Centre "Molecular Structuring of Soft Matter" (CRC1176, A4, B3, C2, C6) and the cluster 3D Matter Made To Order all funded under Germany's Excellence Strategy -2082/1--390761711 are greatly acknowledged for financial contributions. We acknowledge support from the Engineering and Physical Sciences Research Council of the UK (grant EP/P010482/1), from the International Collaborative Research Program of Institute for Chemical Research, Kyoto University (grant # 2020-37 and 2021-37), and from JSPS KAKENHI Grant Number JP20H05840 (Grant-in-Aid for Transformative Research Areas, "Dynamic Exciton"). ZZ acknowledges the financial support from Chinese Scholarship Council (CSC, 201606890009) for his PhD studies.

References

(1) Liu, Y.; Li, C.; Ren, Z.; Yan, S.; Bryce, M. R. All-Organic Thermally Activated Delayed Fluorescence Materials for Organic Light-Emitting Diodes. *Nat. Rev. Mater.* **2018**, *3*, 18020.

(2) Baldo, M. A.; an dY. You, D. F. O.; Shoustikov, A.; Sibley, S.; Thompson, M. E.; Forrest, S. R. Highly Efficient Phosphorescent Emission from Organic Electroluminescent Devices. *Nature* **1998**, *395* (September), 151–154.

(3) Milián-Medina, B.; Gierschner, J. Computational Design of Low Singlet-Triplet Gap All-Organic Molecules for OLED Application. *Org. Electron.* **2012**, *13* (6), 985–991. https://doi.org/10.1016/j.orgel.2012.02.010.

(4) Cui, L. S.; Nomura, H.; Geng, Y.; Kim, J. U. k.; Nakanotani, H.; Adachi, C. Controlling Singlet–Triplet Energy Splitting for Deep-Blue Thermally Activated Delayed Fluorescence Emitters. *Angew. Chemie - Int. Ed.* **2017**, *56* (6), 1571–1575. https://doi.org/10.1002/anie.201609459.

(5) Rajamalli, P.; Chen, D.; Li, W.; Samuel, I. D. W.; Cordes, D. B.; Slawin, A. M. Z.; Zysman-Colman, E. Enhanced Thermally Activated Delayed Fluorescence through Bridge Modification in Sulfone-Based Emitters Employed in Deep Blue Organic Light-Emitting Diodes. *J. Mater. Chem. C* **2019**, *7* (22), 6664–6671. https://doi.org/10.1039/c9tc01498e.

(6) Lays, P.; Chen, D.; Rajamalli, P.; Matulaitis, T.; David, B.; Slawin, A. M. Z.; Jacquemin, D.; Zysman-colman, E.; Samuel, I. D. W. The Use of Pyrimidine and Pyrazine Bridges as a Design Strategy to Improve the Performance of Thermally Activated Delayed Fluorescence Organic Light Emitting Diodes. *ACS Appl. Mater. Interfaces* **2019**, *11*, 45171–45179. https://doi.org/10.1021/acsami.9b16952.

(7) Dias, F. B.; Penfold, T. J.; Monkman, A. P. Photophysics of Thermally Activated Delayed Fluorescence Molecules. *Methods Appl. Fluoresc.* **2017**, *5* (1), 012001. https://doi.org/10.1088/2050-6120/aa537e.

(8) El-Sayed, M. A. The Triplet State: Its Radiative and Nonradiative Properties. *Acc. Chem. Res.* **1968**, *1* (1), 8–16. https://doi.org/10.1021/ar50001a002.

(9) Liu, M.; Komatsu, R.; Cai, X.; Hotta, K.; Sato, S.; Liu, K.; Chen, D.; Kato, Y.; Sasabe, H.; Ohisa, S.; Suzuri, Y.; Yokoyama, D.; Su, S. J.; Kido, J. Horizontally Orientated Sticklike Emitters: Enhancement of Intrinsic Out-Coupling Factor and Electroluminescence Performance. *Chem. Mater.* **2017**, *29* (20), 8630–8636. https://doi.org/10.1021/acs.chemmater.7b02403.

(10) Yokoyama, D.; Sakaguchi, A.; Suzuki, M.; Adachi, C. Horizontal Orientation of Linear-Shaped Organic Molecules Having Bulky Substituents in Neat and Doped Vacuum-Deposited Amorphous Films. *Org. Electron. physics, Mater. Appl.* **2009**, *10* (1), 127–137. https://doi.org/10.1016/j.orgel.2008.10.010.

(11) Xiang, S.; Lv, X.; Sun, S.; Zhang, Q.; Huang, Z.; Guo, R.; Gu, H.; Liu, S.; Wang, L. To Improve the Efficiency of Thermally Activated Delayed Fluorescence OLEDs by Controlling the Horizontal Orientation through Optimizing Stereoscopic and Linear Structures of Indolocarbazole Isomers. *J. Mater. Chem. C* **2018**, *6* (21), 5812–5820. https://doi.org/10.1039/c8tc01419a.

(12) Maeng, J. H.; Ahn, D. H.; Lee, H.; Jung, Y. H.; Karthik, D. Rigid Indolocarbazole Donor Moiety for Highly Efficient Thermally Activated Delayed Fluorescent Device. *Dye. Pigment.* **2020**, 108485. https://doi.org/10.1016/j.dyepig.2020.108485.

(13) Naqvi, B. A.; Schmid, M.; Crovini, E.; Sahay, P.; Naujoks, T.; Rodella, F.; Zhang, Z.; Strohriegl, P.; Bräse, S.; Zysman-Colman, E.; Brütting, W. What Controls the Orientation of TADF Emitters? *Front. Chem.* **2020**, *8* (September), 750. https://doi.org/10.3389/fchem.2020.00750.

(14) Zhang, Z.; Crovini, E.; dos Santos, P. L.; Naqvi, B. A.; Cordes, D. B.; Slawin, A. M. Z.; Sahay, P.; Brütting, W.; Samuel, I. D. W.; Bräse, S.; Zysman-Colman, E. Efficient Sky-Blue Organic Light-Emitting Diodes Using a Highly Horizontally Oriented Thermally Activated Delayed Fluorescence Emitter. *Adv. Opt. Mater.* **2020**. https://doi.org/10.1002/adom.202001354.

(15) Cha, J. R.; Lee, C. W.; Lee, J. Y.; Gong, M. S. Design of Ortho-Linkage Carbazole-Triazine Structure for High-Efficiency Blue Thermally Activated Delayed Fluorescent Emitters. *Dye. Pigment.* **2016**, *134*, 562–568. https://doi.org/10.1016/j.dyepig.2016.08.023.

(16) Park, H. J.; Han, S. H.; Lee, J. Y. A Directly Coupled Dual Emitting Core Based Molecular Design of Thermally Activated Delayed Fluorescent Emitters. *J. Mater. Chem. C* **2017**, *5* (46), 12143–12150. https://doi.org/10.1039/c7tc03133e.

(17) Yong Joo Cho, Sang Kyu Jeon, Sang-Shin Lee, Eunsun Yu, and J. Y. L. Donor Interlocked Molecular Design for Fluorescence-like Narrow Emission in Deep Blue Thermally Activated Delayed Fluorescent Emitters. *Chem.Mater.* **2016**, *28*, 5400–5405.

(18) Cho, Y. J.; Jeon, S. K.; Chin, B. D.; Yu, E.; Lee, J. Y. The Design of Dual Emitting Cores for Green Thermally Activated Delayed Fluorescent Materials. *Angew. Chemie - Int. Ed.* **2015**, *54* (17), 5201–5204. https://doi.org/10.1002/anie.201412107.

(19) Kim, M.; Jeon, S. K.; Hwang, S. H.; Lee, S. S.; Yu, E.; Lee, J. Y. Highly Efficient and Color Tunable Thermally Activated Delayed Fluorescent Emitters Using a "Twin Emitter" Molecular Design. *Chem. Commun.* **2016**, *52* (2), 339–342. https://doi.org/10.1039/c5cc07999c.

(20) Wei, D.; Ni, F.; Wu, Z.; Zhu, Z.; Zou, Y.; Zheng, K.; Chen, Z.; Ma, D.; Yang, C. Designing Dual Emitting Cores for Highly Efficient Thermally Activated Delayed Fluorescent Emitters. *J. Mater. Chem. C* **2018**, *6* (43), 11615–11621. https://doi.org/10.1039/c8tc02849d.

(21) Chen, D.; Kusakabe, Y.; Ren, Y.; Sun, D.; Wada, Y.; Suzuki, K.; Kaji, H.; Zysman-, E. Multichromophore Molecular Design for Efficient Thermally Activated Delayed Fluorescence Emitters with Near-Unity Photoluminescence Quantum Yields. *ChemRxiv* **2021**. https://doi.org/10.1021/acs.joc.1c01101.

(22) Byeon, S. Y.; Kim, J.; Lee, D. R.; Han, S. H.; Forrest, S. R.; Lee, J. Y. Nearly 100% Horizontal Dipole Orientation and Upconversion Efficiency in Blue Thermally Activated Delayed Fluorescent Emitters. *Adv. Opt. Mater.* **2018**, *6* (15), 1701340. https://doi.org/10.1002/adom.201701340.

(23) Sharma, N.; Spuling, E.; Mattern, C. M.; Li, W.; Fuhr, O.; Tsuchiya, Y.; Adachi, C.; Bräse, S.; Samuel, I. D. W.; Zysman-Colman, E. Turn on of Sky-Blue Thermally Activated

Delayed Fluorescence and Circularly Polarized Luminescence (CPL): Via Increased Torsion by a Bulky Carbazolophane Donor. *Chem. Sci.* **2019**, *10* (27), 6689–6696. https://doi.org/10.1039/c9sc01821b.

(24) Kim, M.; Jeon, S. K.; Hwang, S. H.; Lee, S. S.; Yu, E.; Lee, J. Y. Correlation of Molecular Structure with Photophysical Properties and Device Performances of Thermally Activated Delayed Fluorescent Emitters. *J. Phys. Chem. C* **2016**, *120* (5), 2485–2493. https://doi.org/10.1021/acs.jpcc.5b09114.

(25) Schmidt, T. D.; Lampe, T.; Daniel Sylvinson, M. R.; Djurovich, P. I.; Thompson, M. E.; Brütting, W. Emitter Orientation as a Key Parameter in Organic Light-Emitting Diodes. *Phys. Rev. Appl.* **2017**, *8* (3), 37001. https://doi.org/10.1103/PhysRevApplied.8.037001.

(26) Senes, A.; Meskers, S. C. J.; Dijkstra, W. M.; Van Franeker, J. J.; Altazin, S.; Wilson, J. S.; Janssen, R. A. J. Transition Dipole Moment Orientation in Films of Solution Processed Fluorescent Oligomers: Investigating the Influence of Molecular Anisotropy. *J. Mater. Chem. C* **2016**, *4* (26), 6302–6308. https://doi.org/10.1039/c5tc03481g.

(27) Senes, A.; Meskers, S. C. J.; Greiner, H.; Suzuki, K.; Kaji, H.; Adachi, C.; Wilson, J. S.; Janssen, R. A. J. Increasing the Horizontal Orientation of Transition Dipole Moments in Solution Processed Small Molecular Emitters. *J. Mater. Chem. C* **2017**, *5* (26), 6555–6562. https://doi.org/10.1039/C7TC01568B.

(28) Gao, Y.; Hlil, A.; Wang, J.; Chen, K.; Hay, A. S. Synthesis of Homo- And Copoly(Arylene Bicarbazole)s via Nucleophilic Substitution Polycondensation Reactions of NH Groups with Activated Dihalides. *Macromolecules* **2007**, *40* (14), 4744–4746. https://doi.org/10.1021/ma0702750.

(29) Zhang, Q.; Zhuang, H.; He, J.; Xia, S.; Li, H.; Li, N.; Xu, Q.; Lu, J. Improved Ternary Memory Performance of Donor-Acceptor Structured Molecules through Cyano Substitution. *J. Mater. Chem. C* **2015**, *3* (26), 6778–6785. https://doi.org/10.1039/c5tc00839e.

(30) Grimme, S. Density Functional Calculations with Configuration Interaction for the Excited States of Molecules. *Chem. Phys. Lett.* **1996**, *259*, 128–137.

(31) Santos, P. L.; Ward, J. S.; Data, P.; Batsanov, A. S.; Bryce, M. R.; Dias, F. B.; Monkman, A. P. Engineering the Singlet-Triplet Energy Splitting in a TADF Molecule. *J. Mater. Chem. C* **2016**, *4* (17), 3815–3824. https://doi.org/10.1039/c5tc03849a.

(32) Hosokai, T.; Matsuzaki, H.; Nakanotani, H.; Tokumaru, K.; Tsutsui, T.; Furube, A.; Nasu, K.; Nomura, H.; Yahiro, M.; Adachi, C. By Delocalized Excited States. *Sci. Adv.* **2017**, *3* (May), 1603282. https://doi.org/10.1126/sciadv.1603282.

(33) Noda, H.; Nakanotani, H.; Adachi, C. Excited State Engineering for Efficient Reverse Intersystem Crossing. *Sci. Adv.* **2018**, *4* (6), eaao6910. https://doi.org/10.1126/sciadv.aao6910.

(34) Samanta, P. K.; Kim, D.; Coropceanu, V.; Brédas, J. L. Up-Conversion Intersystem Crossing Rates in Organic Emitters for Thermally Activated Delayed Fluorescence: Impact of the Nature of Singlet vs Triplet Excited States. *J. Am. Chem. Soc.* **2017**, *139* (11), 4042–4051. https://doi.org/10.1021/jacs.6b12124.

(35) Wada, Y.; Nakagawa, H.; Matsumoto, S.; Wakisaka, Y.; Kaji, H. Molecular Design Realizing Very Fast Reverse Intersystem Crossing in Purely Organic Emitter. *ChemRix* **2019**, No. 2, 1–21. https://doi.org/10.26434/CHEMRXIV.9745289.V1.

(36) Wada, Y.; Nakagawa, H.; Matsumoto, S.; Wakisaka, Y.; Kaji, H. Organic Light Emitters Exhibiting Very Fast Reverse Intersystem Crossing. *Nat. Photonics* **2020**, No. 14, 643–649. https://doi.org/10.1038/s41566-020-0667-0.

(37) Wang, X.; Yan, Q.; Chu, P.; Luo, Y.; Zhang, Z.; Wu, S.; Wang, L.; Zhang, Q. Analysis on Fluorescence of Dual Excitable Eu(TTA)3DPBT in Toluene Solution and PMMA. *J. Lumin.* **2011**, *131* (8), 1719–1723. https://doi.org/10.1016/j.jlumin.2011.03.061.

(38) Crosby, G. A.; Demas, J. N. Measurement of Photoluminescence Quantum Yields. Review. *J. Phys. Chem.* **1971**, *75* (8), 991–1024. https://doi.org/10.1021/j100678a001.

(39) Song, F.; Xu, Z.; Zhang, Q.; Zhao, Z.; Zhang, H.; Zhao, W.; Qiu, Z.; Qi, C.; Zhang, H.; Sung, H. H. Y.; Williams, I. D.; Lam, J. W. Y.; Zhao, Z.; Qin, A.; Ma, D.; Tang, B. Z. Highly Efficient Circularly Polarized Electroluminescence from Aggregation-Induced Emission Luminogens with Amplified Chirality and Delayed Fluorescence. *Adv. Funct. Mater.* **2018**, *28* (17), 1–12. https://doi.org/10.1002/adfm.201800051.

(40) Kumar, M.; Pereira, L. Mixed-Host Systems with a Simple Device Structure for Efficient Solution-Processed Organic Light-Emitting Diodes of a Red-Orange TADF Emitter. *ACS Omega* **2020**, *5* (5), 2196–2204. https://doi.org/10.1021/acsomega.9b03253.

(41) Vecchi, P. A.; Padmaperuma, A. B.; Qiao, H.; Sapochak, L. S.; Burrows, P. E. A Dibenzofuran-Based Host Material for Blue Electrophosphorescence. *Org. Lett.* **2006**, *8* (19), 4211–4214. https://doi.org/10.1021/ol0614121.

TOC Graphic

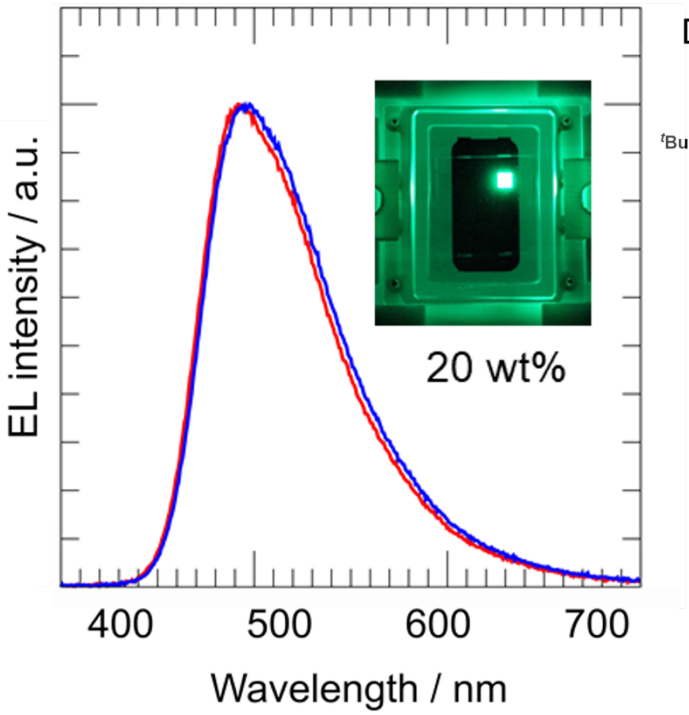

Dual emitter design